Journal of Pharmacokinetics and Pharmacodynamics, Vol. 32, Nos. 5–6, December 2005 (© 2005)
DOI: 10.1007/s10928-005-0019-1

Population Cell Life Span Models for Effects of Drugs Following Indirect Mechanisms of Action[1]

Juan J. Perez-Ruixo,[2,*] Hui C. Kimko,[3] Andrew T. Chow,[3] Vladimir Piotrovsky,[2] Wojciech Krzyzanski,[4] and William J. Jusko[4]

Received February 21, 2005—Final August 25, 2005

Pharmacokinetic/pharmacodynamic (PK/PD) models for hematological drug effects exist that assume that cells are produced by a zero- or first-order process, survive for a specific duration (cell lifespan), and then are lost. Due to the fact that delay differential equations (DDE) are needed for cell lifespan models, their software implementation is not straightforward. Our objective is to demonstrate methods to implement three different cell lifespan models for dealing with hematological drug effects and to evaluate the performance of NONMEM to estimate the model parameters. For the basic lifespan indirect response (LIDR) model, cells are produced by a zero-order process and removed due to senescence. The modified LIDR model adds a precursor pool. The LIDR model of cytotoxicity assumes a three-pool indirect model to account for the cell proliferation with capacity-limited cytotoxicity followed by maturation, and removal from the circulation. A numerical method (method of steps) implementing DDE in NONMEM was introduced. Simulation followed by estimation was used to evaluate NONMEM performance and the impact of the minimization algorithm (first-order method vs. first-order conditional estimation method) and the model for residual variability on the estimates of the population parameters. The FOCE method combined with log-transformation of data was found to be superior. This report provides methodology that will assist in application of population methods for assessing hematological responses to various types of drugs.

KEY WORDS: indirect response models; cell lifespan; delay deferential equations; hematological effects; cytotoxicity.

[1]Part of the contents of this manuscript has been presented as an oral presentation (Perez-Ruixo, JJ; Kimko, HC; Chow, A; Piotrovskij, V. *NONMEM Implementation of Cell Lifespan Models for Hematological Drug Effects*) at XIII meeting of Population Approach Group in Europe (http://www.page-meeting.org/) in Uppsala (Sweden), 2004.

[2]Johnson & Johnson Pharmaceutical Research & Development, Beerse, Belgium.
[3]Johnson & Johnson Pharmaceutical Research & Development, Raritan, NJ, USA.
[4]Department of Pharmaceutical Sciences, School of Pharmacy and Pharmaceutical Sciences, State University of New York at Buffalo, USA.
*To whom correspondence should be addressed. E-mail: jperezru@prdbe.jnj.com

INTRODUCTION

Numerous mathematical models of hematopoiesis have been developed (1,2). Each major hematopoietic process including erythropoiesis (3), granulopoiesis (4), and thrombopoiesis (5) has been modeled and the lifespan concept has been used to control the numbers of cells at various stages. A compartmental approach has been commonly used for a lifespan model where the number of compartments varies. The regulatory role of hematopoietic growth factors was expressed by parameters describing proliferation, differentiation and maturation of progenitor and precursor cells in various stages. These multicompartmental models are of physiological nature where different inputs to the same model can account for a variety of changes in a normal steady-state. However, they require a number of parameters that are not often available while analyzing clinical data.

Maturation of cells is a major reason for prolonged delays between the occurrence of drug action on precursor cells and observed response in the subsequent cell populations. In the absence of any intervention, a lag time in the response vs. time profile corresponds to the maturation time for precursor pools. For hematopoietic cells, the maturation time in bone marrow varies from 2 to 7 days. A common technique to incorporate this maturation time is to apply a series of transit compartments connected via first-order processes with the same rate constant $1/\tau$, where τ is the mean transit time through each compartment (6,7). Another approach to model the delay is simply by introducing the delay time as a model parameter, which can be interpreted as the general lifespan of a specific cell population, that is the time between its entry to and exit from the population.

Mitotic creation of new cells can be accounted for in a model by increasing the number of cells that have the same properties that are characteristic for the cell population. Likewise, cell death can be modeled as a loss of such properties. In addition, the idea of applying aging velocities to cell transport between compartments was introduced previously (8). Basic pharmacodynamic models implementing the cell lifespan as a delay parameter have been previously reported (9, 10), and these have been applied to quantitation of effects of erythropoietin on reticulocytes and red blood cells (RBC) (11–13).

This manuscript describes how to apply the concept of lifespan-driven cell turnover (10,14) to the case where proliferation or chemotherapy-induced degradation rate is stimulated by agents. In the lifespan based indirect response (LIDR) models, the cells corresponding to a certain cell population are eliminated from a compartment not by a first-order process

but by the end of their lifespan, probably due to senescence. Therefore, the cell loss rate is the rate of cell production delayed by the cell lifespan. Consequently, if the production rate is perturbed by an intervention that depends on model variables (e.g. drug effects), then the model is no longer a system of ordinary differential equations (ODE) but a system of delay differential equations (DDE) (15). Additional complexity of LIDR models is in dependence of the cell senescence rate on other cell elimination pathways. For example, if the cells are killed by a cytotoxic drug, the senescence rate has to be corrected by the fraction of cells that survived (14).

NONMEM is a widely used program for pharmacokinetic (PK) and pharmacodynamic (PD) population analysis (16). Like most available programs for PK/PD data analysis this program is not equipped with a DDE solver, but has a robust ODE solver. However, a numerical technique is available to transform any system of DDE to a system of ODE by a step-wise procedure called method of steps (17). The biggest limitation of this method is that, in general, the number of ODE depends on the ratio of the smallest delay time to the overall time range of the data to be solved. With a catenary structure, this limitation does not apply for a DDE system. Therefore, these types of models are naturally used to represent the development of hematopoietic cells.

Our objective is to demonstrate methods to implement the LIDR models of hematopoietic cell populations using the step-wise method to transform the DDE system into an ODE system that can be solved by NONMEM. We analyzed basic LIDR models for drugs that stimulate the production of cells (10), LIDR models with a precursor pool, and LIDR models for cytotoxic effects of anticancer agents (14). We assessed the NONMEM performance for each of these models and provided control streams and example data.

METHODS

Method of Steps

The method of steps allows one to solve virtually any DDE system by transforming it to an ODE system. We demonstrate the application of this method for a system of DDE with one delay time T_1 and a constant initial condition for the time, $-T_1 \leq t < 0$:

$$\frac{dx}{dt} = f(t, x(t), x(t - T_1)) \quad \text{for } t > 0 \tag{1}$$

and

$$x(t) = x_0 \quad \text{for} \quad -T_1 \leq t < 0 \tag{2}$$

where $x = (x_1, \ldots, x_N)$, $x_0 = (x_{01}, \ldots, x_{0N})$, and $f = (f_1, \ldots, f_N)$ are vectors. One can apply the method of steps to transform Eqs. (1) and (2) into a system of ODE (15, 17). This method is based on solving the following equations successively:
for the interval $0 < t \leq T_1$,

$$\frac{dx}{dt} = f(t, x(t), x_0) \tag{3}$$

for the interval $0 < t \leq 2T_1$,

$$\frac{dx_1}{dt} = f(t, x_1(t), x_2(t)) \tag{4}$$

$$\frac{dx_2}{dt} = f(t - T_1, x_2(t), x_0) \tag{5}$$

for the interval $0 < t \leq 3T_1$,

$$\frac{dx_1}{dt} = f(t, x_1(t), x_2(t)) \tag{6}$$

$$\frac{dx_2}{dt} = f(t - T_1, x_2(t), x_3(t)) \tag{7}$$

$$\frac{dx_3}{dt} = f(t - 2T_1, x_3(t), x_0) \tag{8}$$

and so on. The number of differential equations depends on the time interval. For $0 < t \leq t_{max}$, where t_{max} is the maximum time up to which the solution is sought, it is possible to set up a system of ODE such that one of its solutions also solves Eqs. (1) and (2) by introducing new variables

$$y_i(t) = \begin{cases} x(t - iT_1), & \text{if } iT_1 < t \leq t_{max} \\ x_0, & \text{if } t \leq iT_1 \end{cases} \tag{9}$$

One can calculate the maximum number of vector variables necessary to generate the solution of the DDE system Eq. (1) over the time interval $0 \leq t \leq t_{max}$ as $M = \text{INT}(t_{max}/T_1) + 1$, where INT (z) denotes the integer part of the real number z. If x satisfies Eq. (1) for $0 < t \leq t_{max}$ and Eq. (2) for $-T_1 < t \leq 0$, then $y_0, y_1, \ldots, y_{M-1}$ in the interval $0 < t \leq t_{max}$ satisfy the following system of ODE:

$$\frac{dy_0}{dt} = \bar{f}(t, y_0, y_1) \tag{10}$$

$$\frac{dy_1}{dt} = \bar{f}(t - T_1, y_1, y_2) \tag{11}$$

...

$$\frac{dy_{M-1}}{dt} = \bar{f}(t - (I-1)T_1, y_{M-1}, x_0) \tag{12}$$

with the initial conditions

$$y_i(0) = x_0, \quad \text{for } i = 0, 1, \ldots, M-1 \tag{13}$$

The notation, $\bar{f}$, for the right hand sides of Eqs. (10)–(12) has been introduced to accommodate negative times in the right-hand side of Eq. (1),

$$\bar{f}(t, x, y) = \begin{cases} f(t, x, y), & \text{if } 0 \le t \\ 0, & \text{if } t < 0 \end{cases} \tag{14}$$

To avoid writing the NONMEM model equations for negative times, one can assign the lag time to each entry of the vector y_i as:

$$\text{ALAG}_k = i \cdot T_1 \tag{15}$$

where the index k corresponds to the jth entry of the vector y_i. Examples of NONMEM control streams are given in the subsequent sections. Consequently, the solution for the DDE system Eqs. (1) and (2) is represented by a part of the solution of the ODE system Eqs. (10)–(13)

$$x(t) = y_0(t) \tag{16}$$

The solution y_1 is the delayed solution for $x(t - T_1)$, y_2 is the delayed solution for $x(t - 2T_1)$, etc. Although the DDE system shown in Eq. (1) contains one delay time, this method is applicable to a DDE system with many delay times $T_1, \ldots,$ and T_q. The complexity is resolved in the proper indexing of the vector variables y_i where the index i should account for multiple delays T_1, T_2, etc.

The method of steps can yield a solution of the DDE system for any $t > 0$ and not just $0 \le t \le t_{\max}$. This is possible with special "catenary-like" DDE systems:

$$\frac{dx_1}{dt} = f_1(t, x_1) \tag{17}$$

$$\frac{dx_2}{dt} = f_2(t, x_1, x_2, x_1(t - T_1), \ldots, x_1(t - T_q)) \tag{18}$$

$$\frac{dx_3}{dt} = f_3(t, x_1, x_2, x_3, x_1(t - T_1), \ldots, x_1(t - T_q), x_2(t - T_1), \ldots, x_2(t - T_q)) \ldots \tag{19}$$

$$\frac{dx_N}{dt} = f_N(t, x_1, \ldots, x_N, x_1(t - T_1), \ldots, x_1(t - T_q), \ldots, x_{N-1}(t - T_1), \ldots, x_{N-1}(t - T_q)) \tag{20}$$

with the initial conditions in Eq. (2). The basic property of Eqs. (17)–(20) is that the right-hand side of each DDE for x_i depends only on t, the unknown variables proceeding x_i and x_i itself, and the delay unknown variables that proceed x_i. Consequently, starting with x_1 one can solve Eq. (17) and substitute it into Eq. (18). Then Eq. (18) is an ODE for x_2 that can be solved and inserted into Eq. (19). Continuing in this fashion one can gradually reach the equation for x_N and solve it in the same manner. The LIDR models presented below have this catenary-like DDE system property and the method of steps yields the solutions.

Basic LIDR Model

In the basic LIDR model, a population of cell R is controlled by two processes: cell production ($k_{\text{in}}(t)$) and cell loss ($k_{\text{out}}(t)$). The loss process is assumed to be a consequence of natural senescence or conversion to another type of cell. Each cell lives for the same period of time T_{R} and then disappears. This lifespan determines the cell elimination rate. Therefore, the rate of cell loss is the rate of cell production delayed by the time T_{R} (10):

$$k_{\text{out}}(t) = k_{\text{in}}(t - T_{\text{R}}) \tag{21}$$

Consequently, the change in the cell number can be described by

$$\frac{dR}{dt} = k_{\text{in}}(t) - k_{\text{in}}(t - T_{\text{R}}) \tag{22}$$

If the cells are produced at the zero-order rate k_0, and the drug stimulates the production, then (18):

$$k_{\text{in}}(t) = k_0 \cdot \left(1 + \frac{S_{\max} C(t)^{\gamma}}{SC_{50}^{\gamma} + C(t)^{\gamma}}\right) \tag{23}$$

where $C(t)$ is the drug concentration in the cell compartment, $S_{\max}$ is the maximum stimulation, SC_{50} denotes the drug concentration eliciting 50% of the maximum stimulation, and γ is the Hill coefficient.

The one-compartment pharmacokinetic model with first-order elimination was considered to describe $C(t)$:

$$\frac{dA}{dt} = -k_{\text{el}} \cdot A \quad \text{and} \quad A(0) = \text{Dose} \tag{24}$$

where A stands for amount of a drug (which was implemented with volume of distribution of 1, so that $C(t) = A(t)$). Equation (24) has been used for the purposes of this study; however, this method is not limited to monoexponential kinetics as it can easily be accommodated for various pharmacokinetic driving models. Consequently, Eq. (22) describing the basic model becomes

$$\frac{dR}{dt} = k_0 \cdot S(t) - k_0 \cdot S(t - T_{\text{R}}) \tag{25}$$

where $S(t)$ is the abbreviation for the sigmoidal maximum effect model function in Eq. (23). The schematic of the basic LIDR model is presented in Fig. 1a. The baseline equation is (10):

$$R_0 = k_0 \cdot T_{\text{R}} \tag{26}$$

Appendix A shows the NONMEM code implementing the method of steps for the system of DDE Eqs. (24) and (25). Therefore, the system of Eqs. (10)–(12) is described by 3 ODE in Appendix A; the first DE (DADT(1)) describes the time course of the drug-amount, $A(t)$; the second DE (DADT(3)) is for the delayed time course of the drug amount, $A(t - T_{\text{R}})$; and the third DE (DADT(2)) represents the time course of number of cells, $R(t)$. ALAG3 in the NONMEM code was set as T_{R}, because it corresponds to the delay duration. This parameter implements the DDE system to the ODE system to calculate $A(t - T_{\text{R}})$. The baseline value R_0 given by Eq. (26) was used as the initial condition for $R(t)$ and was implemented by setting F2 to R_0. Also, the corresponding AMT at $t = 0$ was set to 1 in the data file. The CALLFL was set to –2 to call

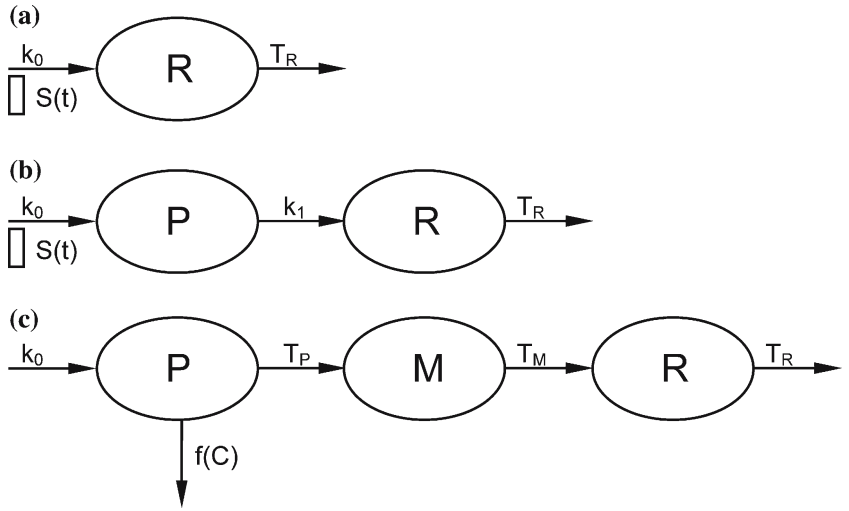

Fig. 1. Diagrams epresenting three lifespan-based models: (a) The basic LIDR model. The cell count response R is produced at a time dependent rate. The cell loss rate is determined by the cell production rate delayed by the cell lifespan T_R. The drug stimulates the production rate (open box). (b) The modified LIDR model with precursor. The precursor cells P are produced at the zero-order rate k_0 and are eliminated at the first-order rate k_1. The cells at the central pool R are eliminated at the rate $k_1 \cdot P$ delayed by their lifespan T_R. Drug stimulates the production rate k_0. (c) The LIDR model of cytotoxic effects of anticancer agents. The precursor cells P and M represent proliferating and maturating cells in bone marrow. Drug irreversibly removes the proliferating cells at a rate that depends on the anticancer agent plasma concentration ($f(C)$). The precursor cells P are produced at the zero-order rate k_0 and those which survive the cytotoxic effect are transformed to the maturating cells after time T_P. The maturation lasts for the time T_M after which the cells are released to the circulation. The lifespan of the cells in the circulation is T_R.

the subroutine PK with every event record and with additional and lagged doses.

Modified LIDR Model with a Precursor Pool

The modified LIDR model that includes a precursor compartment (Fig. 1b) assumes that the population of cells in the central pool R is produced as a consequence of conversion of cells from another population P. The precursor cells, P, are assumed to be produced at the zero-order rate k_0, and transformed to the cells R at the first-order rate k_1. The cells in the central pool are lost after time T_R. The drug is assumed to stimulate the precursor cell production via the Hill function given in Eq. (23). Consequently, the precursor pool is described by the basic IDR model equations (18). The differential equations determining the cell populations P and R are

$$\frac{dP}{dt} = k_0 \cdot S(t) - k_1 \cdot P \tag{27}$$

$$\frac{dR}{dt} = k_1 \cdot P - k_1 \cdot P(t - T_R) \tag{28}$$

The baseline values of P and R can be determined similarly to those for the basic IDR and LIDR models model

$$P_0 = k_0/k_1 \quad \text{and} \quad R_0 = k_0 \cdot T_R \tag{29a,b}$$

Appendix B presents the NONMEM code implementing the method of steps for the system of DDE, Eqs.(24), (27), and (28). The cells in the pool R are delayed by T_R following the cell lifespan model, whereas the cells in the pool P are delayed following the indirect response model. The system of Eqs. (10)–(12) is described by 5 ODE: the first describes $A(t)$, the second $P(t)$, the third $A(t-T_R)$, the fourth $P(t-T_R)$, and the fifth $R(t)$. ALAG3 and ALAG4 were set as T_R. This implements Eq. (14) to the ODE for $A(t - T_R)$, but because the initial condition for $P(t - T_R)$ was nonzero, Eq. (14) was written in its original conditional form where $P(t-T_R) = P_0$ for $t < T_R$. The baseline values P_0 and R_0 given by Eq. (29a,b) were used as the initial condition for P, $P(t - T_R)$, and $R(t)$ and were implemented by setting F2, and F4 to P_0 and F5 to R_0 and the corresponding AMT values at $t = 0$ as 1 in the data file.

LIDR Models of Cytotoxic Effects of Anticancer Agents

The LIDR model of cytotoxic effect of anticancer agents (Fig. 1c) consists of a blood compartment (R) and two precursor compartments (P and M). The hematologic effect R can represent any natural cells including platelet, leukocyte or neutrophil counts. These cells are released to the circulation from the bone marrow in the last stage of their development. The cells that are sensitive to toxic effects of an anticancer agent form the pool P. This compartment contains myeloid progenitor cells in their mitotic phases and possibly other progenitor cells. The cells from the mitotic pool P enter the maturation storage pool M. The cells in P are produced at the zero-order rate (k_0) from the stem cells.

There are two loss processes from the mitotic compartment P: killing by the anticancer agent and the conversion to another cell type (M) after survival in the compartment P. The surviving cells live for the duration of T_P. The killing rate at time t is proportional to the cell number

in the pool P, following the control function, $f(C)$ (19,20), which is non-negative and increases with the plasma concentration, C, of the anticancer drug. If the killing process is saturable (nonlinear), $f(C)$ can be described by a sigmoidal maximum effect model:

$$f(C) = \frac{K_{\max} C^{\gamma}}{KC_{50}^{\gamma} + C^{\gamma}} \tag{30}$$

where $K_{\max}$ is the maximum rate of the killing, KC_{50} denotes the drug concentration eliciting 50% of $K_{\max}$, and γ is the Hill coefficient. The fraction of the cells in the mitotic pool that survived the cytotoxic effect of anticancer agent and is converted to the maturating cells is (14):

$$\mathrm{SF}(t) = \exp\left(-\int_{t-T_{\mathrm{P}}}^{t} f(C(z))dz\right) \tag{31}$$

The number of cells in pool R is determined by:

$$\frac{dR}{dt} = k_0 \cdot \mathrm{SF}(t - T_{\mathrm{M}}) - k_0 \cdot \mathrm{SF}(t - T_{\mathrm{M}} - T_{\mathrm{R}}) \tag{32}$$

The equations for cells in pools P and M are not necessary to calculate the number of cells in the central pool R. The baseline condition for R is

$$R_0 = k_0 \cdot T_{\mathrm{R}} \tag{33}$$

The numerical complexity is in calculating the integral in the conversion rate Eq. (31) with the limits of integration, which depends on the cell lifespans. This can be achieved by introducing a "dummy" variable $\mathrm{Int}(t)$ representing the integral in Eq. (31) such that:

$$\mathrm{SF}(t) = \exp(-(\mathrm{Int}(t) - \mathrm{Int}(t - T_{\mathrm{P}}))) \tag{34}$$

This variable satisfies the following ODE:

$$\frac{d\ \mathrm{Int}}{dt} = f(C(t)) \tag{35}$$

with the zero initial condition,

$$\mathrm{Int}(0) = 0 \tag{36}$$

Because of the presence of delays in Eqs. (32) and (34), Eqs. (32) and (35) form a system of DDE that can be solved using the method of steps.

In Appendix C we present the NONMEM code implementing the method of steps for this system. The delay times are T_M, $T_P + T_M$, $T_M + T_R$ and $T_P + T_M + T_R$ and only the Int(t) variable is delayed. Therefore the system of Eqs. (10)–(12) consists of 9 ODE: the first (DADT(2)) describes A(t-T_M-T_P), the second (DADT(6)) Int A(t-T_M-T_P), the third (DADT(3)) describes A(t-T_M), the fourth (DADT(7)) Int (t-T_M), the fifth (DADT(4)) describes A(t-T_R-T_M-T_P), the sixth (DADT(8)) Int(t-T_R-T_M-T_P), the seventh (DADT(5)) describes A(t-T_R-T_M), the eighth (DADT(9)) Int(t-T_R-T_M), and the ninth (DADT(1)) R(t). ALAG2, ALAG3, ALAG4, ALAG5 were set as T_M+ T_P, T_M, T_R + T_M + T_P, T_R+T_M, respectively. This implements Eq. (14) to the ODE for all delayed variables, Int. The baseline value R_0 given by Eq. (33) was used as the initial condition for $R(t)$ and was implemented by setting F_1 to R_0. The corresponding AMT value at $t = 0$ was set as 1 in the data file.

Evaluation of Performance

For each model a dataset was built to explore the performance. The dataset consisted of 5 cohorts of 25 subjects receiving escalating doses (0.1, 1, 10, 100 and 1000 unit) of a stimulating agent or a cytotoxic drug. In order to minimize the impact of the PK on the PD parameters, it was assumed that the PK parameters were known and the same for all subjects. Therefore, only PD measurements at specific sampling times were simulated according to the model parameters presented in Tables I–III. The sampling times were densely selected to cover all responses. For the basic LIDR model they ranged from 0 to 72 hr (43 time points). For the modified basic LIDR model with precursor the last sampling time was 96 hr (25 time points), and for the LIDR models describing cytotoxic effects the last sampling time was 72 hr (63 time points).

For each model, 250 datasets consisting of individual PD responses for 125 subjects were generated and fitted to the same model that previously was used to generate the data. The Hill coefficient was fixed to 1 and, therefore, it was not evaluated in this study. The magnitude of the inter-individual variability in a certain model parameter was assumed to be independent and modeled according to an exponential model. However, due to the low estimability, the random parameters associated with drug-related parameters for all models ($\omega_{Smax}, \omega_{SC50}, \omega_{Kmax}, \omega_{C50}$) as well as the random system parameters for the model of cytotoxic effects (ω_{TP}, ω_{TR}) were set to 0 both in simulations and subsequent estimation procedures. The simulated cell numbers and model predictions were transformed into natural logarithms, and the residual variability was modeled using an additive error model (transform-both-sides approach—TBS).

Table I. Bias and Precision of the Fixed and Random Effect Parameters for the Basic LIDR Model Obtained by Three Methods of Estimation

		FOCE +TBS(N=182)		FO + TBS (N=113)		FO (N=53)	
Parameters	Simulated values	Bias	Precision	Bias	Precision	Bias	Precision
Fixed effects							
θ_{Smax}	50	−0.10	0.70	−8.80*	1.95	−13.72*	5.66
θ_{SC50}(mg/l)	1	0.06	1.24	−1.67	5.00	−18.60*	10.27
θ_{k0}(10^9cells/l/h)	0.05	0.03	1.76	2.85	1.92	−18.09	30.92
θ_{TR}(hr)	20	0.16	1.72	5.50	2.98	16.81*	5.07
Random effects							
ω_{k0}	20%	−0.55	6.50	6.69	8.03	374.23*	690.40
ω_{TR}	20%	−1.60	6.05	−19.90*	4.63	120.90	435.30
σ	10%	−0.04	0.81	36.21*	7.34	166.92*	221.48

N denotes the number of successful minimizations.
*Significant differences from 0, $p < 0.05$.

Table II. Bias and Precision of the Fixed and Random Effect Parameters for the Modified Basic LIDR Model with a Precursor Pool Obtained by Three Methods of Estimation

		FOCE + TBS (N=250)		FO + TBS (N=250)		FO (N=236)	
Parameters	Simulated values	Bias	Precision	Bias	Precision	Bias	Precision
Fixed effects							
θ_{Smax}	50	−0.17	1.29	−2.59*	1.36	2.31	1.53
θ_{SC50}(mg/l)	1	−0.08	2.99	0.54	3.18	8.03*	3.75
θ_{k0}(10^9 cells/l/hr)	0.5	0.12	0.98	2.32*	1.10	1.43	1.32
θ_{k1}(hr^{-1})	0.05	−0.13	1.90	−0.49	2.17	−3.99	2.74
θ_{TR}(hr)	20	−0.05	2.05	−1.06	1.76	4.07	2.84
Random effects							
ω_{k1}	20%	−0.62	7.29	−2.18	6.98	−3.34	6.91
ω_{TP}	20%	−0.25	6.24	−0.13	6.22	−0.40	6.54
σ	10%	−0.13	1.26	1.93	1.35	7.21*	2.19

N denotes the number of successful minimizations.
*Significant differences from 0, $p < 0.05$.

Table III. Bias and Precision of the Fixed and Random Effect Parameters for the LIDR Model of Cytotoxic Effects of Anticancer Agents with Obtained by Three Methods of Estimation

		FOCE + TBS (N=249)		FO + TBS (N=245)		FO (N=94)	
Parameters	Simulated values	Bias	Precision	Bias	Precision	Bias	Precision
Fixed effects							
θ_{Kmax}	2	0.02	0.36	−11.59*	3.28	−7.79*	74.36
θ_{C50}(mg/l)	30	0.01	0.62	−0.24	2.39	14.53	22.98
θ_{BSL},(10^9 cells)	5	−0.32	1.72	−0.07	1.82	−6.76	24.91
θ_{TP}(hr)	5	−0.03	0.35	12.47*	4.01	18.99*	24.22
θ_{TM}(hr)	10	−0.05	0.40	−3.33*	1.42	−5.43	14.16
θ_{TR}(hr)	5	0.44	2.51	9.14	5.00	34.49*	50.12
Random effects							
ω_{BSL}	20%	−0.27	6.27	−0.66	6.74	307.20	1095.84
ω_{TR}	20%	−1.78	8.36	−3.12	10.30	355.01	1679.49
σ	10%	−0.05	0.75	26.98*	12.13	109.73*	286.54

N denotes the number of successful minimizations.
*Significant differences from 0, $p < 0.05$.

This process was repeated to account for the impact of the two different methods of estimation: first-order (FO) and first-order conditional (FOCE). In addition, an exponential error model was used to account for the residual variability and the results were compared to those obtained by using the FO+TBS and FOCE+TBS. The estimated parameters were recorded from the runs that successfully converged and were used to evaluate performance using bias and precision (21). The mean prediction error was used as a measure of bias for parameter P estimation

$$\mathrm{ME_P} = 100 \cdot \frac{1}{N} \sum_{i=1}^{N} \frac{P_{\mathrm{est},i} - P_{\mathrm{sim,i}}}{P_{\mathrm{sim},i}} \tag{37}$$

where N denotes the number of successful minimizations. The root mean squared prediction error was used as a measure of precision:

$$\mathrm{RMSE_P} = 100 \cdot \sqrt{\frac{1}{N} \sum_{i=1}^{N} \left[\frac{P_{\mathrm{est},i} - P_{\mathrm{sim},i}}{P_{\mathrm{sim},i}} \right]^2} \tag{38}$$

where N denotes the number of successful minimizations. The Student t-test was performed to determine if the bias were significantly different than 0.

RESULTS

Basic LIDR Model

The typical time course of the number of cells in the pool, R, is presented in Fig. 2 as a function of dose. The total of 250 replicates were fitted by three methods FO, FO+TBS, and FOCE+TBS. The number of successful minimizations was 53 (21%), 113 (45%), 182 (73%), respectively. The population means of $\theta_{\mathrm{Smax}}, \theta_{\mathrm{SC50}}, \theta_{\mathrm{k0}}, \theta_{\mathrm{TR}}$, as well as the standard deviations of $\omega_{\mathrm{k0}}, \omega_{\mathrm{TR}}$ for inter-individual variability and σ for residual variability were estimated and compared to the true values. The bias and precision of parameter estimates are presented in Table I.

All fixed effect parameter estimates except θ_{k0}, and random effect parameter estimates except ω_{TR} were significantly biased for the FO method ($p < 0.05$). No estimate was significantly biased or imprecise for the FOCE+TBS method. Bias decreased and precision increased in the order of FO, FO+TBS, FOCE+TBS. Compared to the true value, the most precisely estimated fixed effect parameters obtained by the

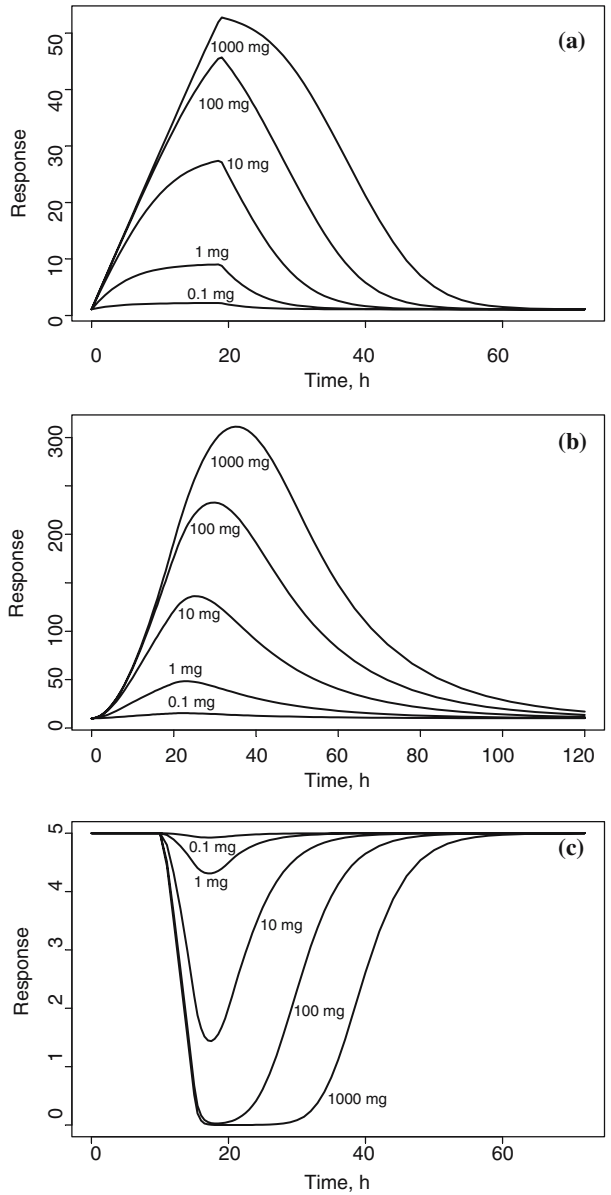

Fig. 2. Response vs. time profiles for three LIDR models. The responses were simulated using the fixed effect models for the indicated dose levels. Panels represent (a) the basic LIDR model, (b) modified basic LIDR model with precursor, and (c) the LIDR for cytotoxic effects of an anticancer agent. The values of the model parameters used for simulations are presented in Tables I–III, respectively.

FOCE+TBS method was θ_{Smax} and the least was θ_{k0}. The random parameter estimates had similar relative biases and precisions, with slight superiority of σ. The frequency distribution of the parameter estimates by the FO method were skewed and none was centered at the true value. Both skewness and bias of the parameter distribution decreased for the FO+TBS method (distributions not shown). The FOCE+TBS method yielded medians for $\theta_{\text{Smax}}, q_{\text{SC50}}, \theta_{\text{k0}}, \theta_{\text{TR}}, \omega_{\text{k0}}$, and ω_{TR} estimates close to true values, and the distributions were symmetrical (see Fig. 3).

Modified LIDR Model with a Precursor Pool

The typical time course of the number of cells in the pool, R, is presented in Fig. 2. as a function of dose. The replicates of 250 such data sets were simulated and each was analyzed using FO, FO+TBS, and FOCE+TBS methods. The numbers of successful minimizations were 236 (94.4%), 250 (100%), and 250 (100%), respectively. The population means of $\theta_{\text{Smax}}, \theta_{\text{SC50}}, \theta_{\text{k0}}, \theta_{\text{k1}}, \theta_{\text{TR}}$, as well as the standard deviations of $\omega_{\text{k1}}, \omega_{\text{TR}}$ and σ were estimated and compared to the true values. The bias and precision of parameter estimates are presented in Table II.

The FO method yielded significant bias in estimating θ_{SC50} and σ, whereas FO+TBS showed significant bias in estimating θ_{Smax} and θ_{k0}. The FOCE+TBS method did not result in a significant bias for any of the parameters. Bias decreased and precision increased in the order of FO, FO+TBS, FOCE+TBS. Compared to the true value, the most precise estimate for the fixed effect parameters obtained by the FOCE+TBS method was θ_{k0} and the least was θ_{SC50}. The random parameter estimates had similar relative biases and precisions, with significant superiority of σ. For the FOCE+TBS method, none of the frequency distributions of the parameter estimates was skewed and all were centered at the true values (see Fig. 4). The distribution of θ_{TR} estimates for the FO method was skewed to the right whereas histograms for remaining parameters were symmetrical. However, for this method, none of the distributions was centered at the true value. The FO+TBS lowered the magnitude of bias, and the distributions were centered at true values only for $\theta_{\text{k1}}, \theta_{\text{SC50}}$, and ω_{TR} (distributions not shown).

LIDR Models of Cytotoxic Effects of Anticancer Agents

The typical time course of the number of cells in the pool, R, is presented in Fig. 2 as a function of dose. The replicates of 250 data sets were simulated and each was analyzed using FOCE+TBS, FO+TBS,

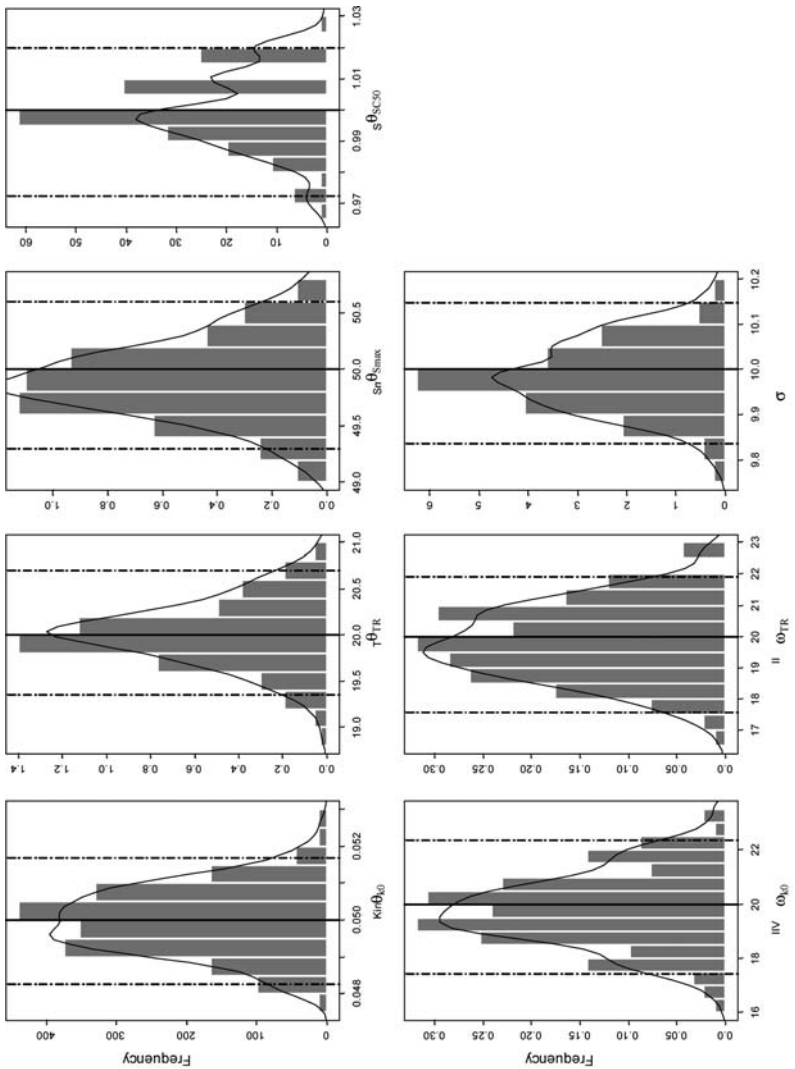

Fig. 3. Histogram and probability distribution function of the estimates for fixed and random PD parameters for the basic LIDR model obtained by the FOCE+TBS method. The solid vertical line represents the true value. Broken vertical lines reflect the 95% confidence intervals.

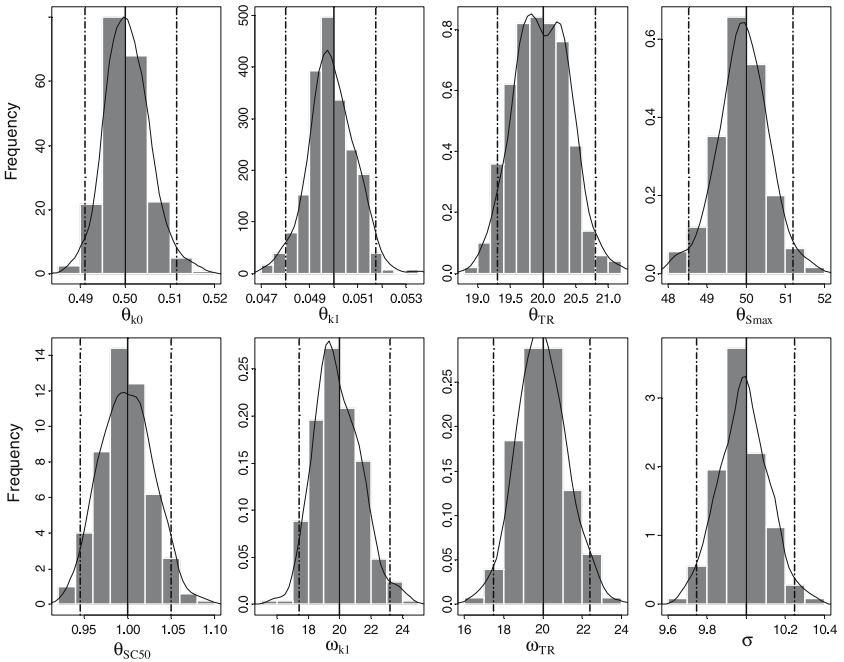

Fig. 4. Histogram and probability distribution function of the estimates for fixed and random PD parameters for the modified basic LIDR model with precursor obtained by the FOCE+TBS method. Vertical lines are defined in Fig. 3.

and FO methods. The numbers of successful minimizations were 249 (99.6%), 245 (98%), and 94 (37.6%), respectively. The population means of $\theta_{\mathrm{Kmax}}, \theta_{\mathrm{C50}}, \theta_{\mathrm{BSL}}, \theta_{\mathrm{TP}}, \theta_{\mathrm{TM}}, \theta_{\mathrm{TR}}$, as well as the standard deviations of $\omega_{\mathrm{BSL}}, \omega_{\mathrm{TR}}$ and σ were estimated and compared to the true values. The bias and precision of parameter estimates are presented in Table III.

The FO method yielded significant bias in estimating $\theta_{\mathrm{Kmax}}, \theta_{\mathrm{TP}}, \theta_{\mathrm{TR}}$, and σ, whereas FO+TBS showed significant bias in estimating $\theta_{\mathrm{Kmax}}, \theta_{\mathrm{TP}}$, θ_{TM}, and σ. The FOCE+TBS method did not result in a significant bias for any of the parameters. Bias decreased and precision increased in the order FO, FO+TBS, FOCE+TBS. Relative to the true value, the most precise estimate for the fixed effect parameters obtained by the FOCE+TBS method was for θ_{Tp} and the least for θ_{BSL}. The random parameter estimates had similar relative biases and precisions, with significant superiority of σ. For the FOCE+TBS method, none of the frequency distributions of the parameter estimates was skewed and all were centered at the true values (see Fig. 5). The distribution of θ_{TP} and θ_{Kmax} estimates for the FO+TBS method was skewed to the right whereas histograms for

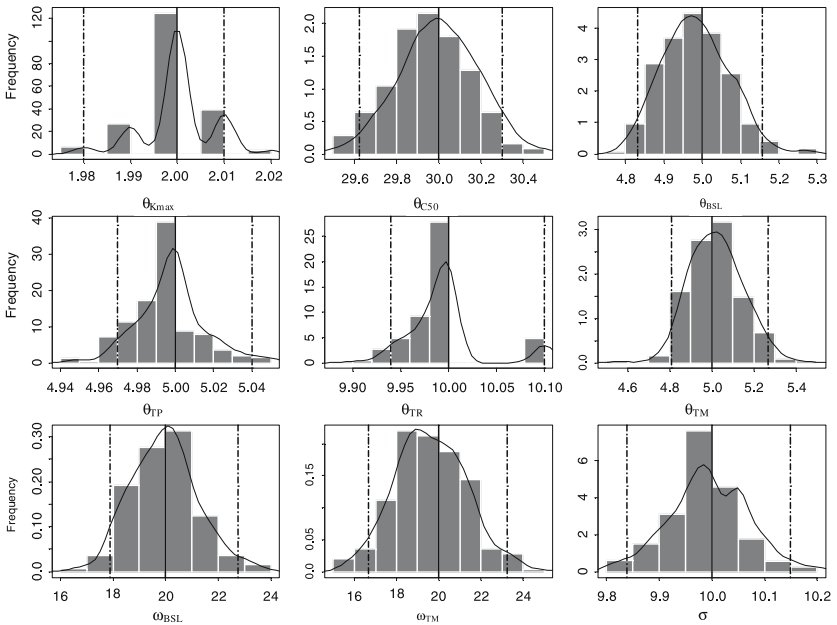

Fig. 5. Histogram and probability distribution function of the estimates for fixed and random PD parameters for the LIDR model of cytotoxic effects of anticancer agents obtained by the FOCE+TBS method. Vertical lines are defined in Fig. 3.

the remaining parameters were symmetrical. However, for the FO method, none of the distributions was centered at the true value (distributions not shown).

DISCUSSION

We present the method of steps in its general form with which any system of DDE can be transformed to a system of ODE. The models are described by Eqs. (17)–(20). For such equations, the number of ODE does not depend on the last observation time unlike for models with feedback mechanisms that are delayed. The number of ODE obtained by the method of steps for models with delayed feedback is a multiple of the original DDE system, and determined by the last observation time and the minimal delay time. An example of a pharmacodynamic model with a delayed feedback can be found elsewhere (12).

If the number of ODE generated by the method of steps exceeds the maximum number allowed by NONMEM, then the method of steps cannot be applied. The basic LIDR model had two DDE that yielded three ODE using the method of steps. The modified basic LIDR with a precursor consisted of three DDE, which required five ODE in the NONMEM code. No numerical instability was reported by the NONMEM ODE solver during the minimization procedure. Therefore, we can conclude that for the types of models described in this manuscript, the method of steps was successfully implemented in NONMEM.

The PK, which is the driving force for the cell lifespan model, was not estimated and no PK variability was introduced in order to minimize the influence of PK variability on estimability of pharmacodynamic parameters. We sampled PD intensively and several single dose regimens were used to increase estimability of fixed effect model parameters. The levels of inter-individual and residual variability were set purposely to moderate values in order not to obscure our objectives but still preserve realistic meaning. For model evaluation, we limited our analysis to precision and bias of fixed and random parameter estimates, leaving out discussion of goodness of fit or parameter correlation issues.

The log transformation of data and model predictions (TBS) has been reported to reduce the bias in the parameter estimates obtained by FO and FOCE methods (22). With this transformation the weighted residual error distribution becomes closer to the normal distribution. For our simulated data with the exponential residual error model (i.e., additive error model in log domain) and TBS, FOCE significantly reduced the bias in nearly all fixed and random parameter estimates for all the models. Therefore, the minimization method FOCE without TBS was not tested in anticipation of a similar improvement after including TBS. As long as the skewness of the residual error distribution following FO or FOCE estimation is observed, TBS is recommended. One might also consider the more general Box–Cox transformation of data and model predictions. However, special care should be taken when selecting the LIDR model to avoid compensating model misspecification by a sophisticated residual error model (22).

From three tested methods of minimization, FOCE+TBS proved to be superior. It was most stable with the lowest number of minimization failures. Both the imprecision and bias of the parameter estimates were smallest. However, the running time necessary to complete minimization was longest of all methods. To ensure the best NONMEM performance, it is recommended to use FOCE+TBS when feasible. The lowest number of successful minimizations for all methods was observed for the basic

LIDR model. Since this model structure was simplest of all discussed cases and the experimental designs similar, one might conclude that minimization failures were caused by random effects. Only two parameters for each model were allowed to vary from subject-to-subject. One can hypothesize that if the model predictions at given time points are sensitive to a parameter with noticeable (CV of 20%) inter-subject variability, then the probability of minimization failure increases. However, more in depth sensitivity analysis is warranted to provide a definite answer for the cause of decreased frequency of successful minimizations for the basic LIDR model.

The modified LIDR model with a precursor differs from the previously introduced model with the cell transport process from the precursor to the blood pool (10). In our model the delay occurs in the precursor cell pool and the system is more complex, presenting more problems with coding the model equations and challenging the NONMEM performance to a greater extent. In a recent paper (13), the modified LIDR with two precursor pools was used for describing reticulocyte tolerance due to precursor depletion. The IDR model with precursor pool catenary linked to compartments where the lifespan concept determine their kinetics gives additional flexibility to the cell lifespan models and has been proven to be a useful strategy to deal with the tolerance phenomena and the cell lifespan concept. A mixture of basic LIDR and modified LIDR models with a precursor was tested in the LIDR model for cytotoxic effects of anticancer agents. All analyzed models had a catenary structure well suitable for application of the methods of steps. For models with the feedback processes (8,12) NONMEM performance can be different and the results presented here might not be valid.

In summary, mixed-effect models implementing cell lifespan concepts can be used to deal with the dynamics of natural cells when hematopoietic growth factors and/or anticancer drugs are administered. LIDR models combined with other PK/PD models add more flexibility to modeling drug responses. The NONMEM performance with the LIDR models is similar to that observed with other PKPD models. The FOCE+TBS method should be used when feasible.

ACKNOWLEDGMENTS

This work was supported in part by Grant No. GM 57980 from the National Institute of General Medical Sciences, NIH.

APPENDIX A: NONMEM code and data file for basic LIDR model

```
$PROB  BASIC LIDR MODEL
$INPUT ID TIME AMT DV CMT
$DATA  MODA.CSV IGNORE=*
$SUB   ADVAN6 TOL=6
$ABBREVIATED DERIV2=NO
$MODEL COMP = CENTRAL
       COMP = (EFFECT,DEFOBS)
       COMP = DCENTRAL
$PK CALLFL = -2
 CL    =  0.25                  ;Clearance
 V     =  1                     ;Volume
 KEL   =  CL/V                  ;Elimination rate constant
 SMAX  =  THETA(1)*EXP(ETA(1))  ;Maximum Stimulatory effect
 SC50  =  THETA(2)*EXP(ETA(2))  ;Drug concentration producing 50% Smax
 KIN   =  THETA(3)*EXP(ETA(3))  ;Zero-order cell production rate
 ALAG3 =  THETA(4)*EXP(ETA(4))  ;Lifespan
 F2    =  KIN*ALAG3             ;Initial condition cell compartment
$DES
 DADT(1) = -KEL*A(1)
 DADT(3) = -KEL*A(3)
 EFF1    = 1 + SMAX*A(1)/(SC50+A(1))
 EFF3    = 1 + SMAX*A(3)/(SC50+A(3))
 DADT(2) = KIN * EFF1 - KIN * EFF3
$ERROR  IPRE = LOG(F+0.0001)
         Y = IPRE + EPS(1)
$THETA (30 50 80)  ;SMAX
       (0 1 10)    ;SC50
       (.01 .05 .1);KIN
       (10 20 30)  ;ALAG1
$OMEGA 0 FIX       ;SMAX
       0 FIX       ;SC50
       0.04        ;KIN
       0.04        ;ALAG1
$SIGMA 0.01
$SIM  (7508)
$EST   MAXEVALS=9990 NSIGDIG=3 NOABORT METHOD=1
$TAB   ID TIME IPRE NOPRINT ONEHEADER
```

The beginning of the data file called by the NONMEM control stream for basic LIDR model.

```
#ID TIME AMT DV  CMT
1   0    10  0   1
1   0    1   0   2
1   0    10  0   3
1   0.25 0   0.1 2
1   0.5  0   1.2 2
```

APPENDIX B: NONMEM code and data file for modified LIDR model with a precursor

```
$PROB  MODIFIED LIDR MODEL WITH A PRECURSOR POOL
$INPUT ID TIME AMT DV CMT
$DATA  MODB.CSV IGNORE=*
$SUB   ADVAN6 TOL=5
$MODEL COMP = CP1  ; PK compartment
       COMP = EF1  ; Precursor Cell compartment
       COMP = CP2  ; PK compartment lagged
       COMP = EF2  ; Precursor Cell compartment lagged
       COMP = EFF  ; Cell compartment
$PK CALLFL = -2
 CL    =  0.25                ;Clearance
 V     =  1                   ;Volume
 KEL   =  CL/V                ;Elimination rate constant
 SMAX  =  THETA(1)*EXP(ETA(1)) ;Maximum Stimulatory effect
 SC50  =  THETA(2)*EXP(ETA(2)) ;Drug concentration producing 50% Smax
 K0    =  THETA(3)*EXP(ETA(3)) ;Zero-order precursor cell production rate
 K1    =  THETA(4)*EXP(ETA(4)) ;First-order precursor cell conversion rate
 ALAG3 =  THETA(5)*EXP(ETA(5)) ;Lifespan
 ALAG4 =  ALAG3
 F2    =  K0/K1               ;Initial condition precursor cell compartment
 F4    =  F2                  ;Initial condition precursor cell compartment
 F5    =  F2 * K1 * ALAG3     ;Initial condition cell compartment
$DES
 DADT(1) = -KEL*A(1)
 EFF1    = 1 + SMAX*A(1)/(SC50+A(1))
 DADT(2) = K0 * EFF1 - K1 * A(2)
 DADT(3) = -KEL*A(3)
 EFF3    = 1 + SMAX*A(3)/(SC50+A(3))
 A4 = F4
 IF (T.GT.ALAG4) A4 = A(4)
 DADT(4) = K0 * EFF3 - K1 * A4
 DADT(5) = K1 * A(2) - K1 * A4
$ERROR  IPRE = LOG(F+0.0001)
        Y = IPRE + EPS(1)
$THETA  (30 50 80)      ;SMAX
        (0 1 10)        ;SC50
        (0.25 0.5 2)    ;K0
        (0.01 0.05 0.25);K1
        (10 20 50)      ;ALAG3
$OMEGA  0 FIX           ;SMAX
        0 FIX           ;SC50
        0 FIX           ;K0
        0.04            ;K1
        0.04            ;ALAG3
$SIGMA  0.01
$SIM   (7509)
$EST    MAXEVALS=9990 NSIGDIG=3 NOABORT METHOD=1
$TAB    ID TIME IPRE NOPRINT ONEHEADER
```

The beginning of the data file called by the NONMEM control stream for the modified LIDR model with a precursor.

```
#ID TIME AMT DV CMT
1   0    10  0  1
1   0    1   0  2
1   0    1   0  3
1   0    10  0  4
1   0    1   0  5
1   0.25 0   1  3
```

APPENDIX C: NONMEM code and data file for LIDR model for cytotoxic effects

```
$PROB  LIDR for Cytotoxic Effects
$INPUT ID TIME AMT DV CMT DOSE
$DATA  ModQ.csv IGNORE=*
$SUB   ADVAN6 TOL=6
$ABBREVIATED DERIV2=NO
$MODEL COMP  = (NEUT1,DEFOBS)        ;Cell Counts
       COMP  = (DELAY2)              ;PK Compartment Delayed ALAG1
       COMP  = (DELAY3)              ;PK Compartment Delayed ALAG2
       COMP  = (DELAY4)              ;PK Compartment Delayed ALAG3
       COMP  = (DELAY5)              ;PK Compartment Delayed ALAG4
       COMP  = (AUC2)                ;AUC COMP2
       COMP  = (AUC3)                ;AUC COMP3
       COMP  = (AUC4)                ;AUC COMP4
       COMP  = (AUC5)                ;AUC COMP5
$PK CALLFL = -2
    CL     = 0.25                 ;Clearance
    V      = 1                    ;Volume
    K10    = CL/V                 ;Elimination rate constant
    KMAX   = THETA(1)*EXP(ETA(1)) ;Maximmum Killing Rate
    C50    = THETA(2)*EXP(ETA(2)) ;Drug concentration producing 50% Kmax
    BSL    = THETA(3)*EXP(ETA(3)) ;Baseline Cell Counts
    TP     = THETA(4)*EXP(ETA(4)) ;Lifespan for Mitotic Cells
    TM     = THETA(5)*EXP(ETA(5)) ;Lifespan for Maturation Phase
    TR     = THETA(6)*EXP(ETA(6)) ;Lifespan for Peripheral Neutrophils
    F1     = BSL
    KIN    = BSL/TR               ;Zero-order Input (from stem cells to mitotic cells)
    ALAG2  = TM+TP                ;T1
    ALAG3  = TM                   ;T2
    ALAG4  = TM+TR+TP             ;T3
    ALAG5  = TM+TR                ;T4
$DES
 DADT(2) = - K10 * A(2)        ;PK Profile Delayed to T=TM+TP
 CP1     = A(2)/V
 EF1     = KMAX*CP1/(C50+CP1) ;Killing Rate Delayed to T=TM+TP
 DADT(6) = EF1                 ;Number of Cells Killed from T=TM+TP

 DADT(3) = - K10 * A(3)        ;PK Profile Delayed to T=TM
 CP2     = A(3)/V
 EF2     = KMAX*CP2/(C50+CP2) ;Killing Rate Delayed to T=TM
 DADT(7) = EF2                 ;Number of Cells Killed from T=TM
 SFP     = EXP(-(A(7)-A(6)))    ;Surviving Fraction of Cells from T=TM to T=TM+TP

 DADT(4) = - K10 * A(4)        ;PK Profile Delayed to T=TP+TM+TR
 CP3     = A(4)/V
 EF3     = KMAX*CP3/(C50+CP3) ;Killing Rate Delayed to T=TP+TM+TR
 DADT(8) = EF3                 ;Number of Cells Killed from T=TP+TM+TR

 DADT(5) = - K10 * A(5)        ;PK Profile Delayed to T=TM+TR
 CP4     = A(5)/V
 EF4     = KMAX*CP4/(C50+CP4) ;Killing Rate Delayed to T=TM+TR
 DADT(9) = EF4                 ;Number of Cells Killed from T=TM+TR
 SFS     = EXP(-(A(9)-A(8)))  ;Surviving Fraction of Cells from T=TM+TR to T=TP+TM+TR
 DADT(1) = KIN*SFP - KIN*SFS  ;Cell Counts Over Time
```

```
$ERROR IPRE = -10
       IF(F.GT.0) IPRE = LOG(F)
       Y = IPRE + EPS(1)

$THETA (0.1 2 50)    ;KMAX
       (0.1 30 100) ;C50
       (1 5 8)       ;BSL
       (2 5 8)       ;TP
       (8 10 20)     ;TR
       (0 5 10)      ;TM
$OMEGA  0 FIX        ;KMAX
        0 FIX        ;C50
        0.04         ;BSL
        0 FIX        ;TP
        0 FIX        ;TR
        0.04         ;TM
$SIGMA 0.01
$SIM (1420708)
$EST MAXEVALS=9990 NSIGDIG=3 NOABORT METHOD=1
$TAB ID TIME IPRE NOPRINT ONEHEADER
```

The beginning of the data file called by the NONMEM control stream for the modified LIDR model with a precursor.

```
#ID    TIME   AMT    DV     CMT
1      0      1      0      1
1      0      1      0      2
1      0      1      0      3
1      0      1      0      4
1      0      1      0      5
1      0.01   0      1      1
```

REFERENCES

1. M. Loeffler H. E. Wichmann. *Structure of the model*. In *Mathematical Modeling of Cell Proliferation: Stem Cell Regulation in Hemopoiesis*, vol. I. H. E. Wichmann, M. Loeffler. (eds.), CRC Press, Inc., Boca Raton, 1985.
2. M. C. Mackey. Mathematical models of hematopoietic cell replication and control. In *The Art of Mathematical Modeling: Case Studies in Ecology, Physiology and Biofluids.* H. G. Othamer, F. R. Adler, M. A. Lewis, and J. C. Dallon (eds.), Prentice Hall, New York, 1996, pp. 149–178.
3. M. Loeffler, K. Pantel, H. Wulff, and H. E. Wichmann. A mathematical model of erythropoiesis in mice and rats, Part 1: Structure of the model. *Cell Tissue Kinet.* **22**:13–30 (1989).
4. S. Schmitz, H. Franke, J. Brusis, and H. E. Wichmann. Quantification of the cell kinetic effects of G-CSF using a model of human granulopoiesis. *Exp. Hematol.* **21**:755–760 (1993).
5. H. E. Wichmann, M. D. Gerhardts, H. Spechtmeyer, and R. Gross. Mathematical model of thrombopoiesis in rats. *Cell Tissue Kinet.* **12**:551–567 (1979).
6. L. A. Harker, L. K. Roskos, U. M. Marzec, R. C. Carter, J. K. Cherry, B. Sundell, E. N. Cheung, D. Terry, and W. Sheridan. Effects of megakaryocyte growth and development factor on platelet production, platelet life span, platelet function in healthy human volunteers. *Blood* **95**:2514–2522 (2000).
7. L. E. Friberg, A. Freijs, M. Sandstrom, and M. O. Karlsson. Semiphysiological model for the time course of leukocytes after varying schedules of 5-fluorouracil in rats. *J. Pharmacol. Exp. Ther.* **295**:734–740 (2000).
8. J. Belair, M. C. Mackey, and J. M. Mahaffy. Age-structured and two-delay models for erythropoiesis. *Math. Biosci.* **128**:317–346 (1995).

9. D. E. Uehlinger, F. A. Gotch, and L. B. Sheiner. A pharmacodynamic model of erythropoietin therapy in uremic anemia. *Clin. Pharmacol. Ther*. **51**:76–89 (1992).
10. W. Krzyzanski, R. Ramakrishnan, and W. J. Jusko. Basic models for agents that alter production of natural cells. *J. Pharmacokin. Biopharm.* **27**:467–489 (1999).
11. R. Ramakrishnan, W. K. Cheung, F. Farrell, L. Joffee, and W. J. Jusko. Pharmacokinetic and pharmacodynamic modeling of recombinant human erythropoietin after intravenous and subcutaneous dose administration in cynomolgus monkeys. *J. Pharmacol. Exp. Ther.* **306**:324–331 (2003).
12. R. Ramakrishnan, W. K. Cheung, M. C. Wacholtz, N. Minton, and W. J. Jusko. Pharmacokinetic and pharmacodynamic modeling of recombinant human erythropoietin after single and multiple doses in healthy volunteers. *J. Clin.Pharmacol.* **44**: 991–1002 (2004).
13. W. Krzyzanski, W. J. Jusko, M. C. Wacholtz, N. Minton, and W. K. Cheung. Pharmacokinetic and pharmacodynamic modeling of recombinant human erythropoietin after multiple subcutaneous doses in healthy subjects. (submitted) *Eur. J. Pharm. Sci.* **26**:295–306 (2005).
14. W. Krzyzanski and W. J. Jusko. Multiple-pool cell lifespan model of haematologic effects of anticancer agents. *J. Pharmacokin. Pharmacodyn.* **29**:311–337 (2002).
15. R. D. Driver. *Ordinary and Delay Differential Equations.* Springer-Verlag, New York, 1977.
16. S. L. Beal and L. B. Sheiner. NONMEM Users Guides. San Francisco: NONMEM Project Group, Univ. Calif. (1989).
17. E. Hairer, S. P. Norsett, and G. Wanner. *Solving Ordinary Differential Equations I: Nonstiff Problems.* Springer, Berlin (1993).
18. N. L. Dayneka, V. Garg, and W. J. Jusko. Comparison of four basic models of indirect pharmacodynamic responses. *J. Pharmacokinet. Biopharm.* **21**:457–478 (1993).
19. W. J. Jusko. Pharmacodynamics of chemotherapeutic effects: dose–time–response relationships for phase-nonspecific agents. *J. Pharm. Sci.* **60**:892–895 (1971).
20. W. J. Jusko. A pharmacodynamic model for cell-cycle-specific chemotherapeutic agents, *J. Pharmacokin. Biopharm.* **1**:175–201 (1973).
21. L. B. Sheiner and S. L. Beal. Some suggestions for measuring predictive performance. *J. Pharmacokin. Biopharm.* **9**:503–512 (1981).
22. P. Girard. Data transformation and Parameter Transformations in NONMEM, The Population Approach Group in Europe Eleventh Meeting, Paris, France, 2002: http://www.page-meeting.org/default.asp?id = 22&keuze = program